

## AUGMENTATION OF VORTEX LIFT BY SPANWISE BLOWING

James F. Campbell\*  
NASA Langley Research Center  
Hampton, Virginia 23665

Abstract

An investigation has been conducted to evaluate the aerodynamic effects associated with blowing a jet spanwise over a wing's upper surface in a direction parallel to the leading edge. Experimental pressure and force data were obtained on wings with sweep angles of 30° and 45° and showed that spanwise blowing aids in the formation and control of the leading-edge vortex and, hence, significantly improves the aerodynamic characteristics at high angles of attack. Full vortex section lift is achieved at the inboard span station with a small blowing rate, but successively higher blowing rates are necessary to attain the full vortex-lift level at increased span distances. Spanwise blowing generates large increases in lift at high angles of attack, improves the drag polars, and extends the linear pitching moment to high lifts; these aerodynamic characteristics are estimated with the leading-edge suction analogy. Integration of the spanwise blowing concept into a fighter aircraft design offers the possibility of increasing specific excess power available for maneuvering at higher load factors.

Symbols

A	Aspect ratio
$a/l$	Notch ratio (see Fig. 9)
b	Span
$c_d, c_l$	Section drag and lift coefficients
$c_r$	Chord at wing-fuselage juncture
$c_{l,p}, c_{l,v}$	Potential and vortex section lift coefficients
$c_{l,tot}$	$c_{l,p} + c_{l,v}$
$C_{D,L}$	Aerodynamic drag-due-to-lift coefficient
$C_L$	Aerodynamic lift coefficient
$C_m$	Aerodynamic pitching-moment coefficient
$C_{L,o}$	Aerodynamic lift coefficient without blowing
$C_{L,p}$	Potential lift coefficient
$C_{L,tot}$	Sum of potential and vortex lift coefficients
$C_\mu$	Nozzle momentum coefficient, $\dot{w} V_j / g q_\infty S$

\*Head, Applied Aerodynamics Section, Subsonic-Transonic Aerodynamics Division. Associate Fellow, AIAA.

$C_T$	Nozzle thrust coefficient, static thrust/ $q_\infty S$
$\Delta C_P$	Difference between upper and lower surface pressure coefficients
$\Delta C_L$	Jet-on lift minus jet-off lift
d	Nozzle diameter
g	Gravity
h	Height of nozzle center line above wing surface
LE	Leading edge
$M_\infty$	Free-stream Mach number
$q_\infty$	Free-stream dynamic pressure
S	Wing reference area
$V_j$	Jet velocity due to isentropic expansion to free-stream static pressure
$V_\infty$	Free-stream velocity
$\dot{w}$	Nozzle-air weight flow
$x_n$	Chordwise distance of nozzle from LE of wing root chord ( $c_r$ )
y	Spanwise distance, measured from model plane of symmetry
$\alpha$	Angle of attack
$\alpha_d$	Angle of attack where measured lift departs from theoretical full vortex-lift curve
$\Lambda_{LE}$	Sweep angle of wing leading edge

Introduction

On thin, highly sweptback wings at moderate-to-high angles of attack, the flow is characterized by a leading-edge separation which forms a stable vortex over the wing and provides large vortex-lift increments. This characteristic of slender wings, of the supersonic cruise type, has been understood for many years. However, for moderately swept wings that have higher aspect ratios and are suitable for fighter aircraft, vortex breakdown occurs at low  $\alpha$ 's. Thus, the wing does not achieve the large vortex-lift increments that are desirable for subsonic maneuvering. These trends are illustrated in Figure 1, which shows the effect of leading-edge sweep on the lift of flat-plate delta wings at  $\alpha = 20^\circ$ .

A promising technique for enhancing the leading-edge vortex and effectively delaying vortex breakdown to higher angles of attack is that of spanwise

blowing. This concept consists of blowing a discrete jet spanwise over the wing's upper surface in a direction essentially parallel to the leading edge. The interaction of this jet flow with the separated flow from the wing leading edge results in the formation and control of a leading-edge vortex, with a subsequent increase in lift. Some original research related to this concept was performed by Werlé<sup>1</sup> and Cornish<sup>2</sup> who demonstrated the control of separated flow regions by transverse blowing. The additional work reported by Dixon et al.<sup>3-5</sup> and Bradley et al.<sup>6</sup> applied the concept to different types of lifting surfaces, such as wings, leading- and trailing-edge flaps, and rudders.

In order to supplement this previous research, two wind-tunnel test programs were conducted to determine the effects of spanwise blowing on wings of interest for fighter aircraft applications, that is, where the wings have moderate sweep angles and moderate-to-high aspect ratios. The first wind-tunnel investigation obtained wing-surface pressure distributions on a trapezoidal wing with a leading-edge sweep angle ( $\Lambda_{LE}$ ) of  $44^\circ$ . Lift, drag, and pitching moment were measured in the second test program on delta, arrow, and diamond wing planforms having  $\Lambda_{LE}$  of  $30^\circ$  and  $45^\circ$ . These tests were performed at a free-stream Mach number of about 0.2 with spanwise blowing from the fuselage only (no ducting in the wings). Data were acquired for a range of angle of attack and jet thrust coefficient.

While specific information about these pressure and force tests is contained in References 7 and 8, respectively, the current paper will summarize some of the research highlights that illustrate the effects of spanwise blowing on the wing's surface pressure distribution, spanwise development of vortex section lift, longitudinal aerodynamic characteristics, angle of attack for vortex breakdown, and specific excess power available for maneuvering.

### Results and Discussion

The objective of blowing spanwise on moderately swept wings is to artificially induce spanwise flow gradients similar to those that appear naturally on highly swept wings,<sup>9-12</sup> such as the delta wing sketched in Figure 1. The flow gradients resulting from blowing are favorable for the formation and control of the leading-edge vortex,<sup>13</sup> as is illustrated in the flow visualization photograph in Figure 2. In the following sections, an effort is made to examine the effects of this complicated jet-vortex flow system on wing pressures and forces.

#### Pressure Tests

The wing-body model utilized for the pressure tests is illustrated in Figure 3 and had a trapezoidal wing with a leading-edge sweep of  $44^\circ$ , an aspect ratio of 2.5, and a taper ratio of 0.2. In addition, the wing had no twist, camber, or dihedral and had a circular arc airfoil section (measured streamwise) with sharp leading and trailing edges. The wing thickness ratio was 6% at the fuselage-wing junction and varied linearly to 4% at the wing tip. The upper and lower surfaces of the wing were instrumented with 140 pressure orifices arranged in chordwise rows at six different span locations.

The tests were conducted in the Langley high-speed 7- by 10-foot wind tunnel at a Mach number of 0.26, and a Reynolds number of  $5.2 \times 10^6$  per meter. Data were obtained for a range of model angle of attack and jet blowing rate for the model without fixed transition. Although a variety of nozzle orientations were examined in Reference 7, the present paper discusses only those data that were obtained with  $h/d = 0.835$ ,  $x_n/c_r = 0.23$ , and  $\Lambda_n = 44^\circ$ .

The primary nozzle parameter that is used herein to identify various jet blowing rates is the jet thrust coefficient,  $C_T$ . This coefficient uses the static nozzle thrust which was obtained as a function of plenum pressure by calibrating the nozzles. Additional details concerning the tests can be obtained from Reference 7.

Wing-Pressure Field. Detailed pressure distributions are presented in Reference 7 and show that spanwise blowing results in significant effects on the wing upper-surface pressure field with little effect on the lower-surface pressures and at high  $\alpha$ 's as opposed to low  $\alpha$ 's. A schematic of the wing pressure field is presented in Figure 4 for  $\alpha = 24^\circ$  and illustrates some of the primary features of the spanwise blowing process.

The attached flow theory is presented in Figure 4 to show what the pressure distribution might be if the flow remained attached at the leading edge. This attached flow condition is represented by the subsonic theory from Reference 14 and is characterized by negatively increasing  $\Delta C_p$  as the leading edge is approached. The experimental data obtained with no blowing ( $C_T = 0$ ) show that the flow cannot negotiate the sharp leading edge and, therefore, separates. In fact for this  $\alpha$ , the  $\Delta C_p$  values are essentially constant which is indicative of separated flow over the entire upper surface.

Spanwise blowing ( $C_T = 0.12$ ) results in significant decreases in  $\Delta C_p$  at the inboard span station and near the wing leading edge. These high suction pressures are a result of the formation of a strong leading-edge vortex, where the flow reattaches to the wing surface at some point aft of the jet flow. At larger  $2y/b$ , the jet-vortex system weakens which results in decreases in the peak pressure near the leading edge and a spreading of the influence over all of the wing section. Reference 7 showed that larger  $C_T$  values increased  $-\Delta C_p$  as well as the spanwise extent of the jet's effect. This suggests that the jet will have the most beneficial effect at that point where the jet and vortex are close to their respective origins, that is, where the jet flow is strong enough to result in vortex rollup and the vortex is still close to the wing surface. These pressure results are similar to those obtained on a rectangular flat plate in Reference 3. The pressure distributions obtained with blowing appear to be similar to those obtained on highly swept delta wings which have a natural (no blowing required) leading-edge vortex.

Section Forces. The chordwise pressure distributions were numerically fitted with a cubic spline and then integrated to obtain the section forces (Ref. 7 also includes section pitching moments). The effects of spanwise blowing on section lift

curves are presented in Figure 5 for the wing span station  $2y/b = 0.5$ . These data show that spanwise blowing increases  $c_l$  throughout the  $\alpha$  range, the largest effect occurring for the largest  $C_T$  and at high  $\alpha$ , where section stall has occurred with no blowing ( $C_T = 0$ ). The nonlinearity in  $c_l$  versus  $\alpha$  that results when there is blowing is typical of sections developing vortex lift.

To better interpret these experimental results, theoretical estimates of the section lift characteristics were made by using the leading-edge suction analogy developed by Polhamus.<sup>15</sup> The basic assumptions which are used in Reference 15 to apply the suction analogy to a wing with a fully developed leading-edge vortex are assumed to apply here on a sectional basis. Accordingly, for a section with no leading-edge suction, the potential and vortex section lifts are given by:

$$c_{l,p} = k_p \sin \alpha \cos^2 \alpha \quad (1)$$

$$c_{l,v} = k_v \sin^2 \alpha \cos \alpha \quad (2)$$

where the total lift is

$$c_{l,tot} = c_{l,p} + c_{l,v} \quad (3)$$

The terms  $k_p$  and  $k_v$  are defined as

$$k_p = c_{l\alpha} \quad (4)$$

and

$$k_v = \frac{c_t}{\cos \Lambda_{LE} \sin^2 \alpha} = \frac{c_s}{\sin^2 \alpha} \quad (5)$$

where  $c_t$  and  $c_s$  are the section thrust- and suction-force coefficients, respectively. Because of their dependence on section properties, the parameters  $k_p$  and  $k_v$  are functions of spanwise location. The parameters  $c_t$ ,  $c_s$ , and  $c_{l\alpha}$  were determined at different span stations on the trapezoidal wing by the lifting surface theory of Reference 16. Since Reference 16 is a linear theory,  $k_v$  was calculated by using  $\alpha^2$  in Equation (5) instead of  $\sin^2 \alpha$ .

The theoretical estimates for section lift with no vortex lift ( $c_{l,p}$ ) and with full vortex lift ( $c_{l,tot}$ ) are shown in Figure 5. With no blowing, the section has little or no leading-edge vortex flow. The dashed line represents the estimated section lift that would result if the leading-edge vortex was fully established and has essentially the same lift-curve slopes as the data with blowing. The lift values are estimated reasonably well if the jet-induced camber effect, noted at  $\alpha = 0^\circ$ , is accounted for. This induced camber effect is dependent on  $C_T$  as well as the  $2y/b$  station (see Ref. 7), and has been observed in other investigations.<sup>3,5</sup>

So far, the data have shown that the amount of sectional vortex lift generated by spanwise blowing is dependent on  $C_T$ ,  $2y/b$ , and  $\alpha$ . One question that should be considered is what value of  $C_T$

does it take to achieve the full vortex-lift level at a given span station? This is demonstrated in Figure 6 where  $c_l$  is plotted as a function of  $C_T$  for the span station at  $2y/b = 0.5$  and  $\alpha = 24^\circ$ . Increasing the jet blowing rate increases  $c_l$  from the basic wing lift value up to, and beyond, the full vortex-lift level estimated by the suction analogy. For this particular span station, a  $C_T$  of about 0.08 is required to achieve the full vortex lift. The data of Reference 7 indicate that, as you might expect, progressively higher values of  $C_T$  are required to obtain this lift level at larger span distances. The trends discussed for Figure 6 are also demonstrated in Figure 7, which presents the spanwise variation of section lift for a range of  $C_T$  values with the model at  $\alpha = 24^\circ$ . One of the interesting aspects of these results is the change in the section lift distribution across the span that results because of spanwise blowing. Increases in the blowing rate results in progressive changes in the shape of the  $c_l$  distribution from the distribution with no blowing, which in this case is typical of a wing with separated upper-surface flow, to the  $c_l$  distribution estimated by the suction analogy. At the higher blowing rates, the section lift values on the inboard portion of the wing are higher than the theoretical estimates. This jet-induced effect, coupled with available vortex lift on the outboard portion of the wing, suggests that higher blowing rates than those used in this test will produce even higher lift levels.

The results of Figures 4-7, suggest that blowing spanwise from the fuselage is a jet-decay problem,<sup>5</sup> which implies that the development of the leading-edge vortex and the associated vortex section lift are strongly dependent on the local jet and vortex flow properties as well as the free-stream velocity. As a matter of reference, the wing and jet geometries of the current study are such that the jet flow must penetrate almost 62 nozzle-exit diameters to reach the wing tip. The resulting decay of the jet velocity is large enough to have a significant effect on the formation of the leading-edge vortex.

The effect of spanwise blowing on the section induced-drag characteristics is presented in Figure 8 for  $2y/b = 0.5$ . It is observed that blowing improves the drag polars, particularly at high  $c_l$ . Estimates for these polars were obtained by taking the section normal force to be the resultant section force, which should be appropriate for the zero LE suction assumption. The theory provides reasonable predictions of induced-drag for the configuration with and without blowing. At high  $c_l$ , the measured  $c_d$  is lower than the predicted level, which is consistent with the lift results discussed in Figure 5.

#### Force Tests

The wind-tunnel model utilized for the force tests is illustrated in Figure 9 and consisted of a body-of-revolution fuselage with delta, arrow, and diamond wing planforms having  $\Lambda_{LE}$  of  $30^\circ$  and  $45^\circ$ . The wings were flat plates having sharp leading edges and no tip chord. The aspect ratio, reference wing area, and notch ratio are listed in Table I for all of the wing configurations. The origin of the stability axis system is defined at 25% of the mean aerodynamic chord for each wing.

Table I. Wing Geometry for Force Tests

Planform	$\Lambda_{LE} = 30^\circ$			$\Lambda_{LE} = 45^\circ$		
	A	S, m <sup>2</sup>	a/l	A	S, m <sup>2</sup>	a/l
Delta	6.93	0.412	0	4.00	0.479	0
Arrow	9.24	.309	.25	5.33	.359	.25
Diamond	5.54	.515	-0.25	3.20	.599	-0.25

The tests were conducted in the General Dynamics Low-Speed Wind Tunnel at a Mach number of 0.2 and a Reynolds number of  $4.6 \times 10^6$  per meter. The sweep angle for the spanwise blowing nozzles corresponded to the wing leading-edge sweep angle. Various chordwise and vertical nozzle positions were investigated in Reference 8 and resulted in the position,  $x_n/c_r = 0.4$  and  $h/d = 1.5$  used for the family of wings. The jet momentum coefficient  $C_{\mu}$  is used herein to correlate the effects of blowing. Further details of these tests can be obtained from Reference 8.

**Aerodynamic Characteristics.** The effects of spanwise blowing on the aerodynamic lift characteristics of the  $30^\circ$  and  $45^\circ$  swept delta-, arrow-, and diamond-wing configurations are illustrated in Figures 10 and 11. These data show only the aerodynamic effects of spanwise blowing, since the thrusting effects have been subtracted out. The reader is referred to Reference 8 for the total forces and moments obtained on all of the wing planforms.

The data in Figures 10 and 11 were obtained for a range of  $C_{\mu}$  values and show that spanwise blowing has a very favorable effect on the lift characteristics, the primary benefits occurring at moderate-to-high angles of attack. Increasing the blowing rate increases the maximum  $C_L$ , as well as the angle of attack where this maximum lift is achieved. These high- $\alpha$  lift trends would be expected from the pressure results discussed in the first part of this paper.

The theoretical lift curves that are shown in the figures were obtained by using the leading-edge suction analogy,<sup>15</sup> which estimates potential lift (dashed line) by assuming that no vortex lift is developed on the wing, and total lift (solid line) by assuming that full vortex lift is achieved. Comparing these theoretical lift results with the experimental data shows that, with no blowing, the wings develop a small amount of vortex lift at low angles of attack, but no vortex lift at higher  $\alpha$ 's. Blowing tends to enhance the development of the leading-edge vortex so that vortex breakdown is delayed and vortex lift is generated. Increasing the blowing rate results in increases in the vortex-lift contribution until the full vortex-lift level is achieved.

At the higher blowing rates, the measured lifts are higher than the estimated values, which is due to jet-induced effects. At low angles of attack, several studies<sup>3,7,8</sup> have associated this interference lift with an "effective" camber

increase. Investigation of the current data showed that the  $C_L$  at  $\alpha = 0^\circ$  increased with increases in  $C_{\mu}$  for all of the wing planforms, and that this increment of lift was not necessarily constant throughout the angle-of-attack range. If the  $C_L$  value at  $\alpha = 0^\circ$  is added to the vortex-lift theoretical values, the adjusted theory yields good predictions for the experimental lifts and therefore provides a theoretical upper bound for the lifts that can be expected due to spanwise blowing for the range of  $C_{\mu}$  values investigated here.

The effects of spanwise blowing on drag-due-to-lift and pitching moment for the  $45^\circ$  delta wing are presented in Figure 12 and typify the results obtained with the other wing planforms. As can be seen, blowing improves the drag polars and extends the linear pitching moment to higher  $C_L$ 's. The experimental data compare favorably with the drag polar and pitching-moment curve estimated by the leading-edge suction analogy.<sup>15,17</sup> It is observed that at low-to-moderate lifts, the drag-due-to-lift data are lower than the zero-suction vortex-lift polar, and, in fact, approach the full-suction polar given by  $C_L^2/\pi A$ . The wing apparently develops a sizable leading-edge suction force without blowing. This may seem unreasonable since the wing has a beveled sharp leading edge, but the flat-plate model is apparently thick enough to allow some amount of thrust recovery. The drag-due-to-lift effects noted here for the  $45^\circ$  swept wing are appropriately larger for  $30^\circ$  swept planforms.<sup>8</sup> Bradley<sup>6</sup> has indicated that these results may be duplicated with small LE flap deflections and used in conjunction with vortex-lift augmentation to improve the drag polar.

#### Lift Effectiveness

The percentage increase in lift that is generated by spanwise blowing on the  $45^\circ$  delta wing is presented in Figure 13, where the parameter  $C_L/C_{L,0}$  is the lift with blowing on divided by the lift with blowing off. The data indicate that for a given  $C_{\mu}$ ,  $C_L/C_{L,0}$  increases with increase in  $\alpha$  until a maximum is obtained. The angle of attack where this maximum occurs is between  $25^\circ$  and  $30^\circ$ , depending on the value of  $C_{\mu}$ , and corresponds to the  $\alpha$  where maximum  $C_L$  is reached in the lift curves of Figure 11. Higher values of  $C_{\mu}$  result in larger percentage gains in lift as evidenced by the 25% increase obtained with  $C_{\mu} = 0.04$  and the 70% increase with  $C_{\mu} = 0.31$ .

In order to get some idea of the gain in lift that theoretically might be expected on the  $45^\circ$  delta wing, the leading-edge suction analogy<sup>15</sup> was used to calculate  $C_{L,tot}/C_{L,p}$  and  $C_{L,tot}/C_{L,0}$  through the  $\alpha$  range. These parameters represent two ways of estimating full vortex-lift gains and are seen to vary with angle of attack in a manner consistent with the experimental data. The difference in these estimates that are observed at high  $\alpha$ 's result because  $C_{L,0}$  becomes substantially less than  $C_{L,p}$ .

Perhaps a more appropriate way to judge the lifting efficiency of spanwise blowing is by examining the lift augmentation ratio,  $\Delta C_L/C_{\mu}$ . The effect of  $\alpha$  and  $C_{\mu}$  on this parameter is presented in Figure 14. Increasing  $\alpha$  increases the augmentation ratio from the minimum value at  $\alpha = 0^\circ$  (this

value would be zero if there were no jet-induced camber effect) to a maximum value at angles of attack from  $25^\circ$  to  $30^\circ$  (depending on  $C_{\mu}$ ). The largest augmentation ratio of 7 was obtained with the lowest  $C_{\mu}$  value, which means that spanwise blowing generates seven times the lift that would be obtained if the jet were vectored downward (perpendicular to the free stream). Increasing the blowing rate decreases the lifting efficiency of spanwise blowing, a trend that is typical of most jet augmentation systems. These data suggest that spanwise blowing becomes more effective in producing lift than thrust vectoring at angles of attack above about  $13^\circ$  to  $16^\circ$  (depending on  $C_{\mu}$ ). These results are typical of the other planform configurations although the magnitudes may change somewhat.

The effect of sweep angle on the jet-induced lift is shown in Figure 15 for delta wings at  $\alpha = 21^\circ$ , where the data for the  $60^\circ$  delta were obtained from the investigation by Bradley and Wray.<sup>18</sup> The results show that substantially more lift is generated by spanwise blowing on wings with lower sweep angles. The reason, of course, is related to the amount of vortex flow on the wing before blowing is applied. At  $\alpha = 21^\circ$ , the  $60^\circ$  delta wing has a sizable amount of natural vortex lift as noted by the estimates of  $C_{L,tot}/C_{L,0}$  in this figure and by the lift trends discussed in Figure 1.

#### Leading-Edge Suction Recovery Boundary

Since the amount of vortex lift achieved by a wing is directly related to the vortex-breakdown phenomenon, it is useful to examine the effects of spanwise blowing on the leading-edge suction recovery boundaries for delta wings. Figure 16 shows the change in  $\alpha_d$  with wing aspect ratio, where  $\alpha_d$  is the angle of attack at which the experimental lift values begin to depart from the theoretical curve for full vortex lift (see insert). This departure can occur because of vortex bursting at the wing trailing edge or vortex asymmetry<sup>15</sup> for delta wings with very low aspect ratios. The region below the hashed curves represents the combinations of aspect ratios and angles of attack where the leading-edge suction is completely recovered as the vortex normal force. Spanwise blowing extends the boundary so that larger departure angles of attack are achieved for a given aspect ratio. Similar results were recently published by Scruggs and Theisen.<sup>19</sup> It is noted that in order to obtain the  $\alpha_d$  values presented in Figure 16 for  $C_{\mu} = 0.3$ , the jet-induced lift at  $\alpha = 0^\circ$  was subtracted out of the lift curve data presented in Figure 11.

Specific Excess Power. Although the spanwise blowing concept has demonstrated large beneficial aerodynamic effects, the true feasibility test is the integration of the spanwise thrust into the complete fighter aircraft design. Considerable work is necessary to obtain the desired spanwise blowing rates without severely penalizing the aircraft's main-engine thrust system, and to assure that the fighter with spanwise blowing is more maneuverable than the fighter without spanwise blowing. An attempt to demonstrate the possible effects of spanwise blowing on aircraft performance is made in Figure 17, where the specific excess power available for maneuvering is presented as a function of load factor for the  $45^\circ$  delta-wing configuration.

For demonstration purposes, an engine thrust and weight are assumed for the "aircraft," where the standard engine thrust is reduced by  $C_{\mu}q_{\infty}S$  when spanwise blowing is utilized. The lift and drag forces that are used here are the total loads measured on the delta-wing configuration,<sup>8</sup> and therefore include the spanwise-blowing thrust components in the lift and drag directions.

The results show that spanwise blowing increases the specific excess power at load factors above 1, and allows higher load factors to be attained before reaching the lift limit. These trends suggest that the improvements in the aerodynamic characteristics at high lifts are larger than the reductions in thrust associated with spanwise blowing. Although this illustrates a potential application to maneuvering aircraft, the practical aspects of propulsion integration and engine technology must be examined before the spanwise blowing concept can be exploited.

#### Concluding Remarks

An investigation has been conducted to determine the aerodynamic effects associated with blowing spanwise on wings of interest for fighter aircraft. This study summarizes the results of two wind-tunnel test programs,<sup>7,8</sup> which were performed to obtain surface-pressure distributions on a  $44^\circ$  swept trapezoidal wing, and lift, drag, and pitching-moment data on delta, arrow, and diamond wing planforms having leading-edge sweeps of  $30^\circ$  and  $45^\circ$ .

The results of the pressure tests indicate that spanwise blowing has significant effects on the upper-surface pressure field at high angles of attack, where the largest suction pressures occur at the inboard span station near the wing leading edge, and diminish outboard. The sectional effects of spanwise blowing are strongly dependent on angle of attack, jet thrust coefficient, and span location, the largest effects occurring at the highest angles of attack, thrust coefficients, and on the inboard portion of the wing. Full vortex section lift, as estimated by the leading-edge suction analogy, is achieved at the inboard span station with a small blowing rate, but successively higher blowing rates are necessary to attain the full vortex-lift level at increased span distances.

The results of the force tests on the family of wing planforms show that spanwise blowing generates large increments in lift at high angles of attack, improves the drag polars, and extends the linear pitching moment to high lifts. The leading-edge suction analogy provides good predictions for the aerodynamic characteristics that were obtained for the wings with a fully developed leading-edge vortex. A 70% increase in lift was realized on the  $45^\circ$  delta wing with a jet momentum coefficient of 0.3; the lift effectiveness was shown to be even greater for wings with lower sweep angle. Spanwise blowing increases the angle of attack where the leading-edge suction is completely recovered as vortex normal force, and offers the possibility of increasing specific excess power available for maneuvering at higher load factors.

References

<sup>1</sup>Werlé, H., "Division and Coming Together of Fluid Flows," La Rech. Aeron. No. 79, 1960.

<sup>2</sup>Cornish, J. J., III., "High Lift Applications of Spanwise Blowing," ICAS Paper No. 70-09, Seventh ICAS Congress, Rome, Sept. 1970.

<sup>3</sup>Dixon, C. J., "Lift Augmentation by Lateral Blowing Over a Lifting Surface," AIAA Paper No. 69-193, Feb. 1969.

<sup>4</sup>Dixon, C. J., "Lift and Control Augmentation by Spanwise Blowing Over Trailing-Edge Flaps and Control Surfaces," AIAA Paper No. 72-781, Aug. 1972.

<sup>5</sup>Dixon, C. J., Theisen, J. G., and Scruggs, R. M., "Theoretical and Experimental Investigations of Vortex-Lift Control by Spanwise Blowing," Experimental Research LG73ER-0169, Vol. I, Sept. 1973.

<sup>6</sup>Bradley, R. G., Whitten, P. D., and Wray, W. O., "Leading-Edge-Vortex Augmentation in Compressible Flow," AIAA Paper No. 75-124, Jan. 1975.

<sup>7</sup>Campbell, J. F., "Effects of Spanwise Blowing on the Pressure Field and Vortex-Lift Characteristics of a 44° Swept Trapezoidal Wing," TN D-7907, 1975, NASA.

<sup>8</sup>Bradley, R. G., Smith, C. W., and Wray, W. O., "An Experimental Investigation of Leading-Edge Vortex Augmentation by Blowing," CR-132415, April 1974, NASA.

<sup>9</sup>Wentz, W. H., Jr., and Kohlman, D. L., "Wind Tunnel Investigations of Vortex Breakdown on Slender Sharp-Edged Wings," CR-98737, 1969, NASA.

<sup>10</sup>Bartlett, G. E., and Vidal, R. J., "Experimental Investigation of Influence of Edge Shape on the Aerodynamic Characteristics of Low Aspect Ratio Wings at Low Speeds," Journal of Aeronautical Sciences, Vol. 22, No. 8, Aug. 1955, pp. 517-533, 588.

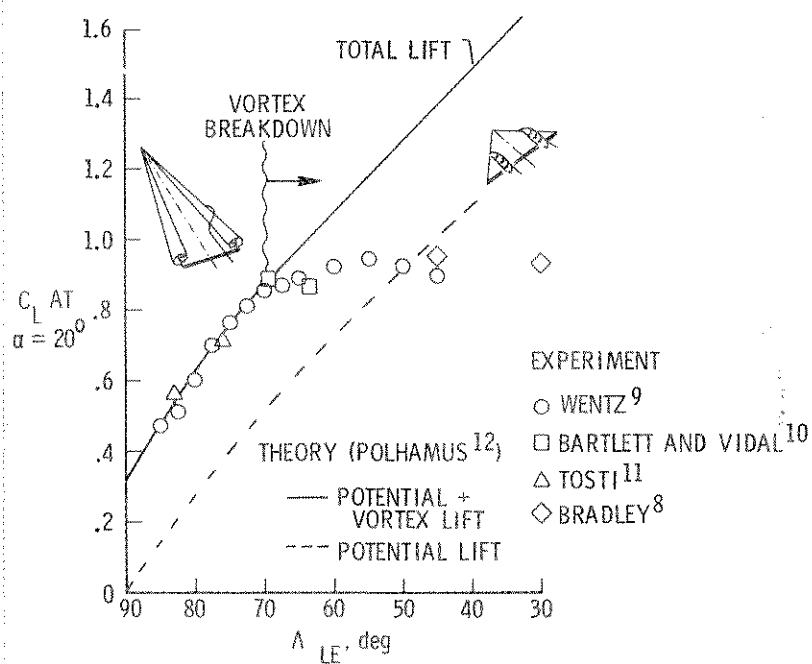


Figure 1. Lift capability of delta wings at  $\alpha = 20^\circ$ .

<sup>11</sup>Tosti, Louis P., "Low-Speed Static Stability and Damping-in-Roll Characteristics of Some Swept and Unswept Low-Aspect-Ratio Wings," TN 1468, 1947 NACA.

<sup>12</sup>Polhamus, E. C., "Charts for Predicting the Subsonic Vortex-Lift Characteristics of Arrow, Delta, and Diamond Wings," TN D-6243, April 1971, NASA.

<sup>13</sup>Erickson, G. E., and Campbell, J. F., "Flow Visualization of Leading-Edge Vortex Enhancement by Spanwise Blowing," TM X-72702, July 1975, NASA.

<sup>14</sup>Woodward, F. A., "An Improved Method for the Aerodynamic Analysis of Wing-Body-Tail Configurations in Subsonic and Supersonic Flows," CR-2228, 1973, NASA.

<sup>15</sup>Polhamus, E. C., "Predictions of Vortex-Lift Characteristics by a Leading-Edge Suction Analogy," Journal of Aircraft, Vol. 8, No. 4, April 1971, pp. 193-199.

<sup>16</sup>Margason, R. J., and Lamar, J. E., "Vortex-Lattice FORTRAN Program for Estimating Subsonic Aerodynamic Characteristics of Complex Planforms," TN D-6142, 1971, NASA.

<sup>17</sup>Lamar, John E., and Gloss, Blair B., "Prediction of Subsonic Aerodynamic Characteristics on Interacting Lifting Surfaces With Separated Flow Around Sharp Leading and Side Edges Using Vortex Lattice Methodology," TN D-7921, 1975, NASA.

<sup>18</sup>Bradley, R. G., and Wray, W. O., "A Conceptual Study of Leading-Edge Vortex Enhancement by Blowing," Journal of Aircraft, Vol. 11, No. 1, Jan. 1974, pp. 34-38.

<sup>19</sup>Scruggs, R. M., and Theisen, J. G., "Transonic Buffet Response Testing and Control," Proceedings for the Symposium on Unsteady Aerodynamics, U.S. Air Force Office of Scientific Research and University of Arizona, Tucson, Arizona, March 19, 1975.

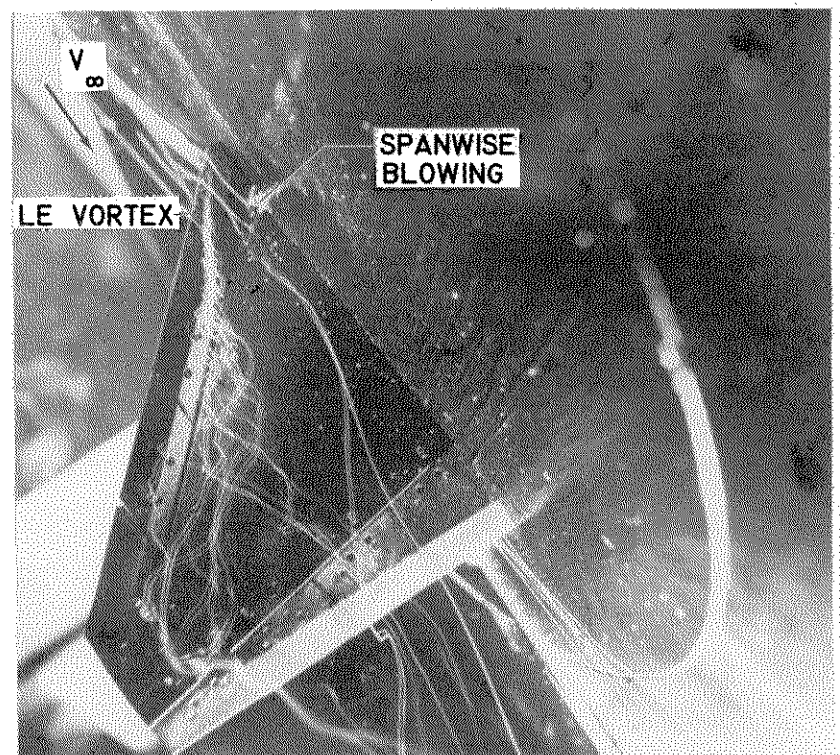


Figure 2. Photograph of a leading-edge vortex enhanced by spanwise blowing on a 44° trapezoidal wing at  $\alpha = 20^\circ$  (from Ref. 13).

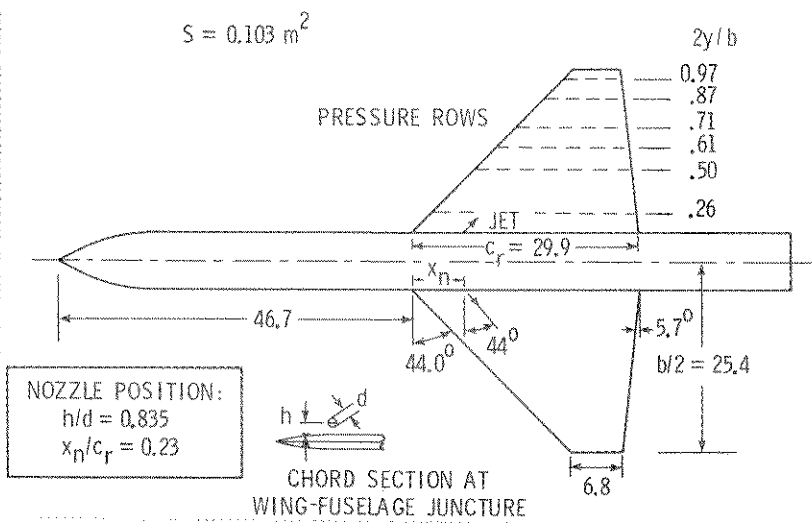


Figure 3. Model geometry for pressure tests (all dimensions are in centimeters).

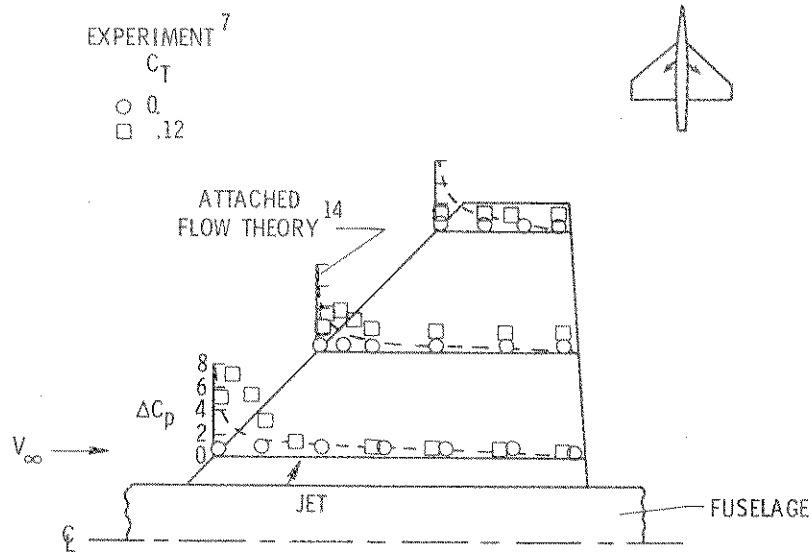


Figure 4. Schematic of wing pressure field for  $\alpha = 24^\circ$ .

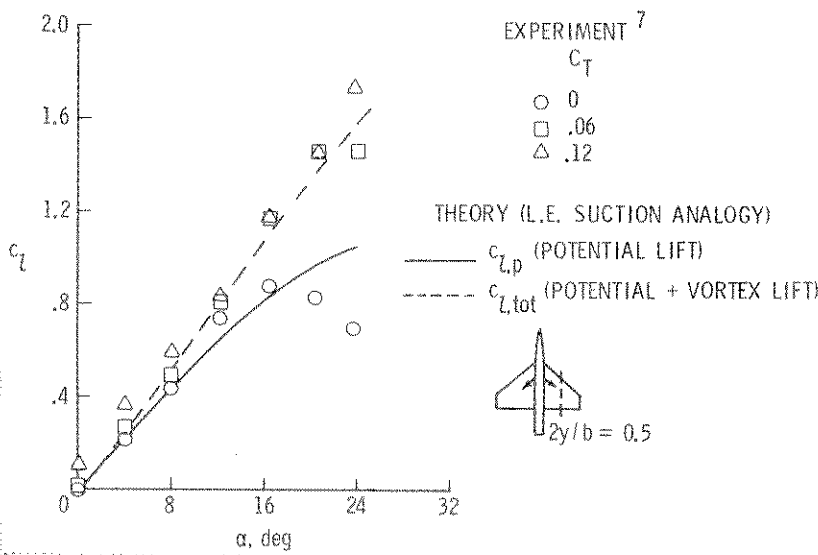


Figure 5. Effect of spanwise blowing on section lift curves at  $2y/b = 0.5$ .

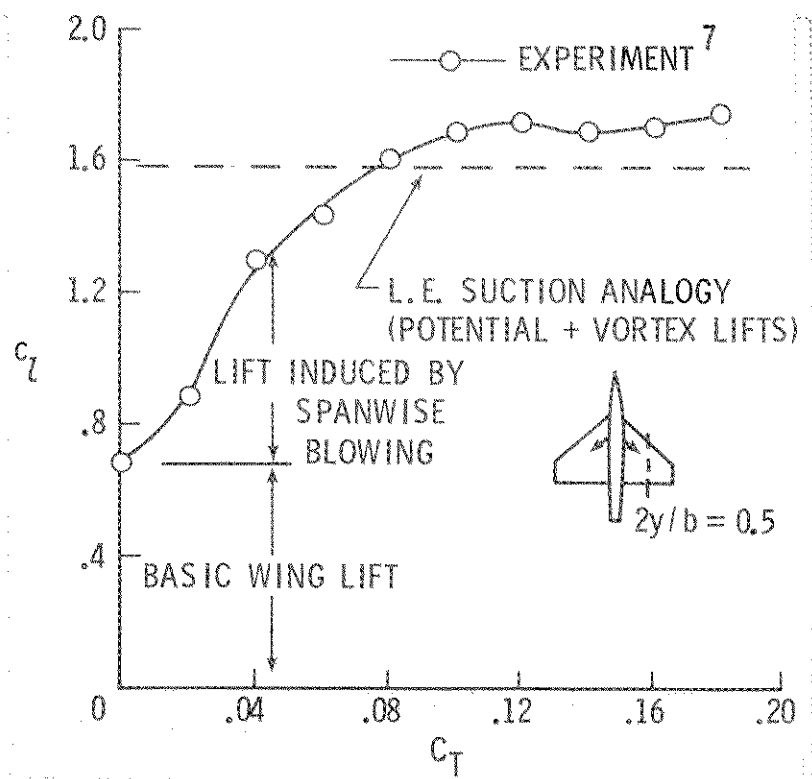


Figure 6. Variation of section lift with  $C_T$  for  $\alpha = 24^\circ$  and  $2y/b = 0.5$ .

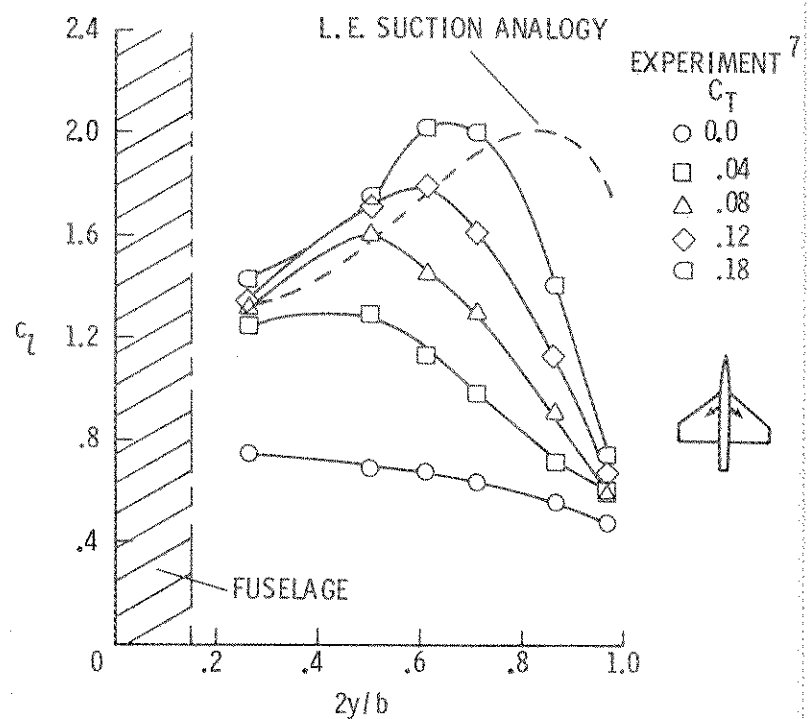


Figure 7. Effect of  $C_T$  on spanwise variation of section lift for  $\alpha = 24^\circ$ .

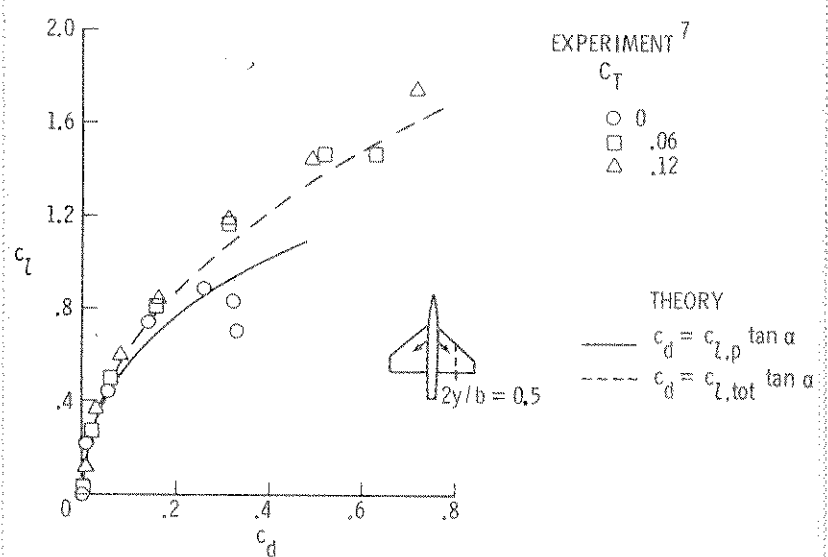


Figure 8. Effect of spanwise blowing on section induced-drag characteristics at  $2y/b = 0.5$ .

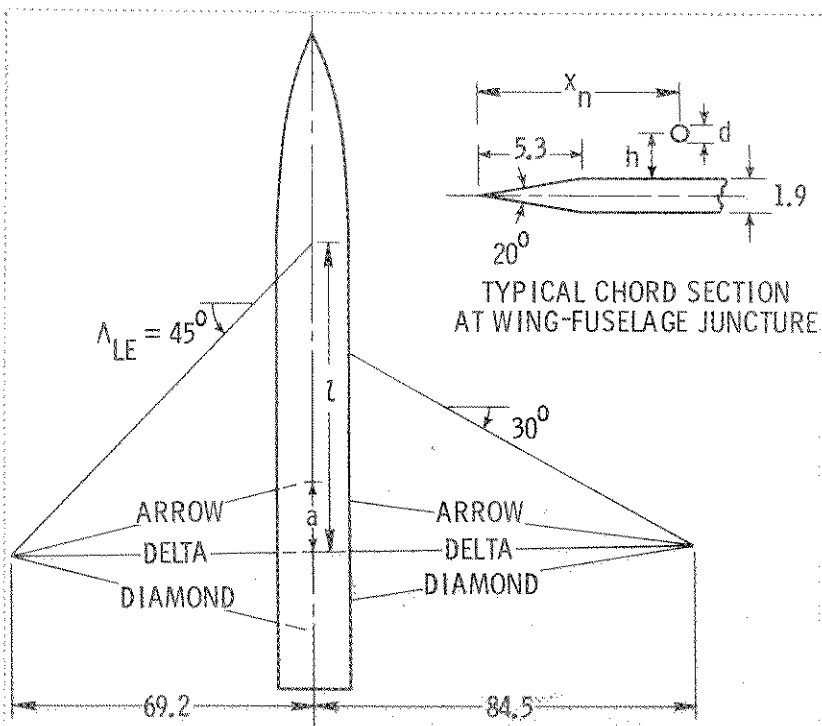


Figure 9. Model geometry for force tests (all dimensions are in centimeters).

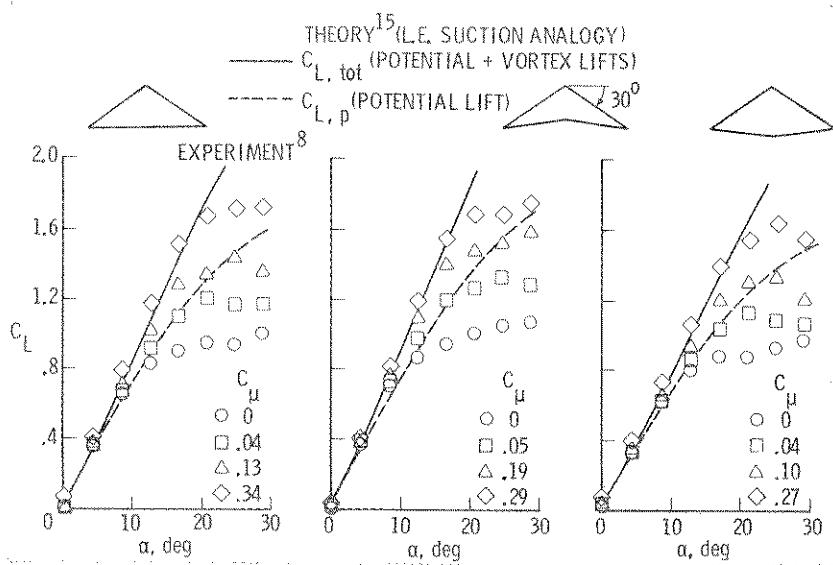


Figure 10. Effect of spanwise blowing on aerodynamic lift characteristics of 30° swept delta, arrow, and diamond wings.

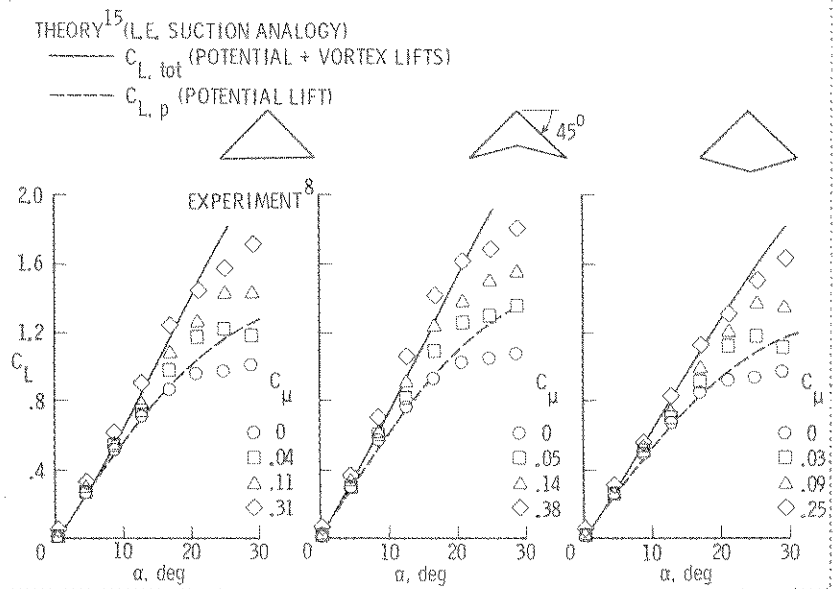


Figure 11. Effect of spanwise blowing on aerodynamic lift characteristics of 45° swept delta, arrow, and diamond wings.

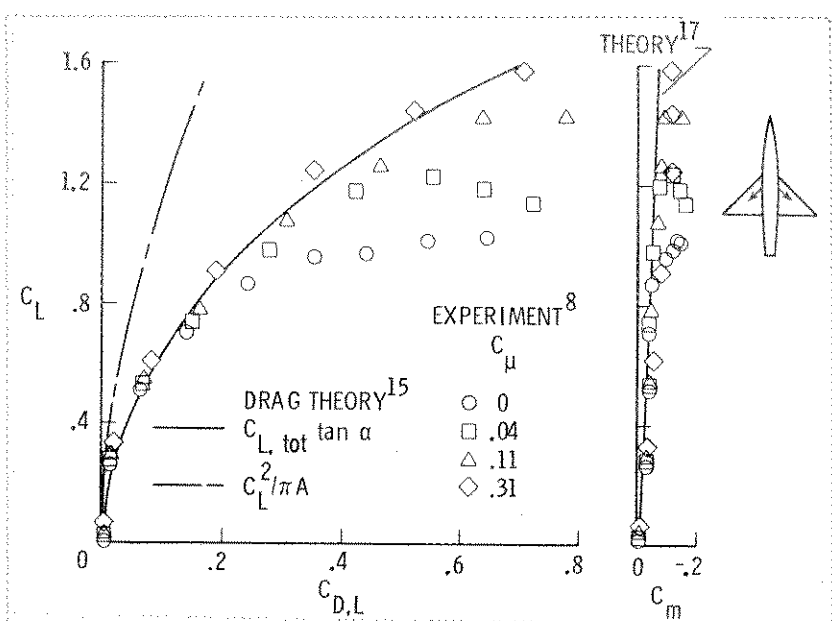


Figure 12. Effect of blowing on drag and pitching moment of the 45° delta wing.

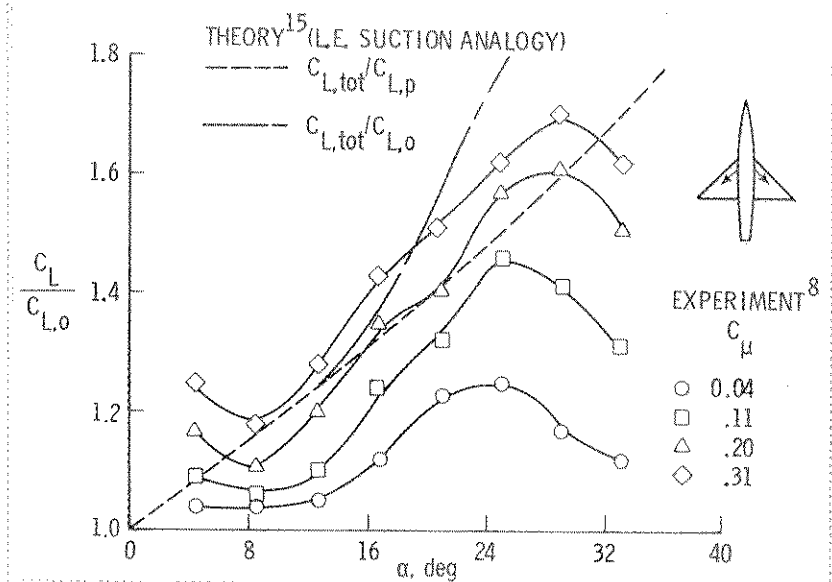


Figure 13. Effect of  $\alpha$  and  $C_\mu$  on the lift effectiveness of blowing on the 45° delta wing.

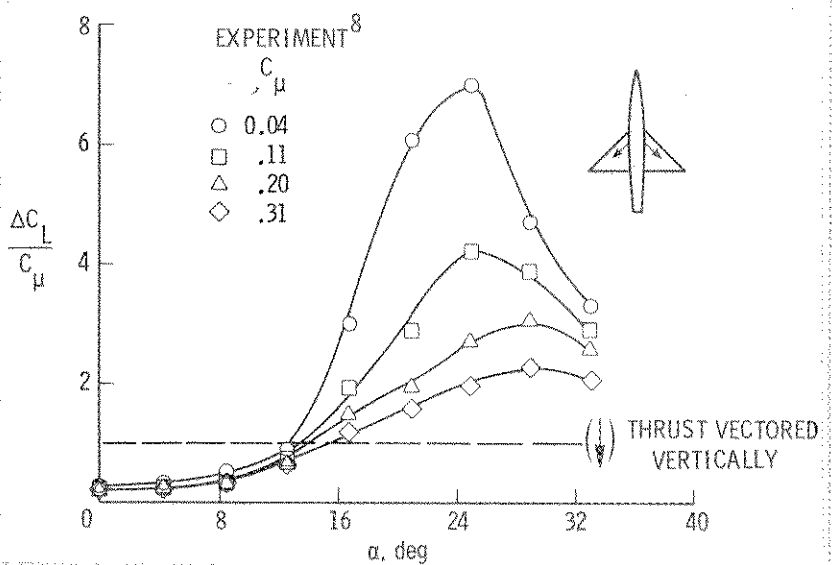


Figure 14. Effect of  $\alpha$  and  $C_\mu$  on lift augmentation ratio for the 45° delta wing.

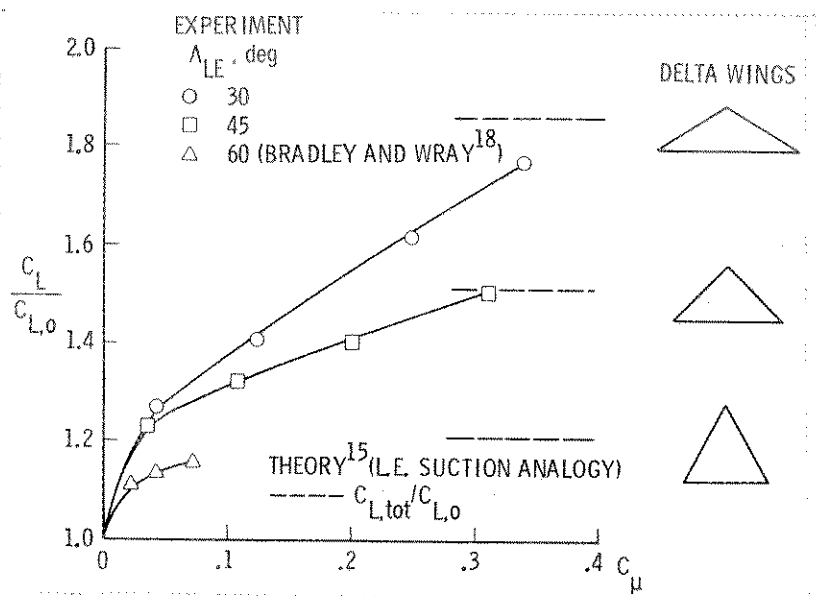


Figure 15. Effect of  $\Lambda_{LE}$  on the lift effectiveness of blowing on delta wing planforms at  $\alpha = 21^\circ$ .

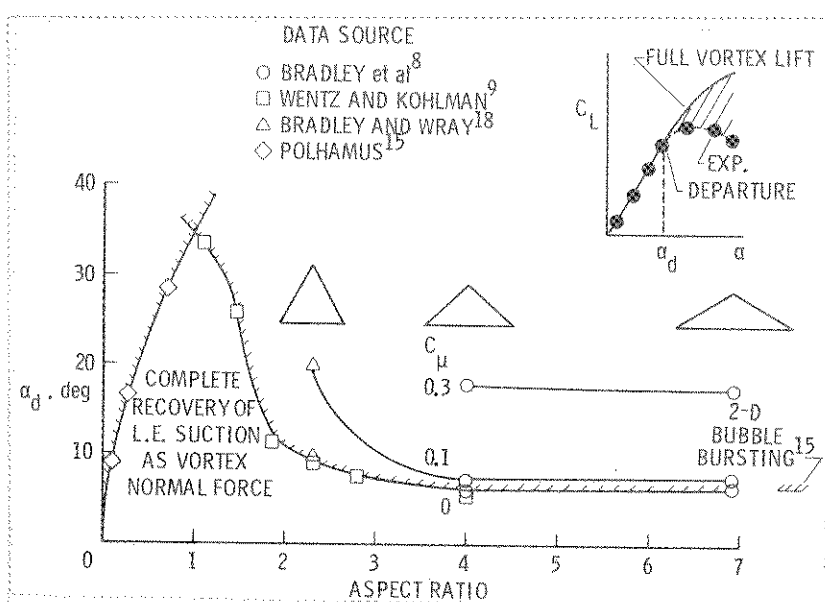


Figure 16. Effect of spanwise blowing on leading-edge suction recovery boundaries for delta wings.

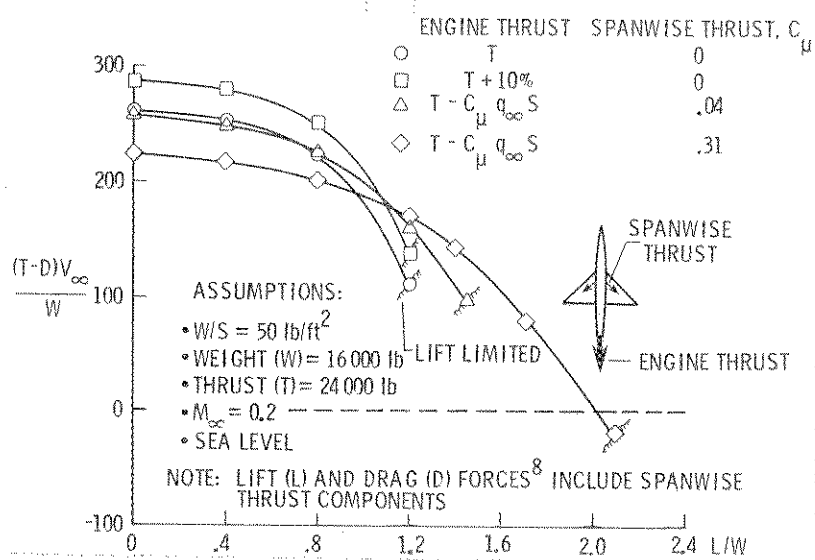


Figure 17. Effect of spanwise blowing on specific excess power available for maneuvering the 45° delta-wing configuration.